CORTEX 166 (2023) 322–337

Available online at www.sciencedirect.com

ScienceDirect

Journal homepage: www.elsevier.com/locate/cortex

Single Case Report

White matter tract disconnection in Gerstmann's syndrome: Insights from a single case study

Mariagrazia Ranzini [a,1,*], *Giulio Ferrazzi* [b,1], *Daniela D'Imperio* [c], *Andreina Giustiniani* [c], *Laura Danesin* [c], *Valentina D'Antonio* [d], *Elena Rigon* [c], *Luisa Cacciante* [c], *Jessica Rigon* [e], *Francesca Meneghello* [e], *Andrea Turolla* [f], *Antonino Vallesi* [g,h], *Carlo Semenza* [g,h,2] *and Francesca Burgio* [c,2]

[a] *Department of General Psychology (DPG), University of Padova, Italy*
[b] *Philips Healthcare, Milan, Italy*
[c] *IRCCS San Camillo Hospital, Lido of Venice, Italy*
[d] *Villa Salus Hospital, Mestre, Italy*
[e] *UOC Cure Primarie - Distretto 3, Mirano - Dolo, AULSS 3, Serenissima, Italy*
[f] *Department of Biomedical and Neuromotor Sciences, University of Bologna, Italy*
[g] *Department of Neuroscience (DNS), University of Padova, Italy*
[h] *Padova Neuroscience Center, University of Padova, Italy*

ARTICLE INFO

Article history:
Received 10 September 2022
Reviewed: 31 October 2022
Revised 17 February 2023
Accepted 18 May 2023
Action Editor Michel Thiebaut de Schotten
Published online 27 June 2023

Keywords:
Gerstmann's syndrome
Optic ataxia
stroke
Lesion Mapping
White matter tract disconnection

ABSTRACT

It has been suggested that Gerstmann's syndrome is the result of subcortical disconnection rather than emerging from damage of a multifunctional brain region within the parietal lobe. However, patterns of white matter tract disconnection following parietal damage have been barely investigated. This single case study allows characterising Gerstmann's syndrome in terms of disconnected networks. We report the case of a left parietal patient affected by Gerstmann's tetrad: agraphia, acalculia, left/right orientation problems, and finger agnosia. Lesion mapping, atlas-based estimation of probability of disconnection, and DTI-based tractography revealed that the lesion was mainly located in the superior parietal lobule, and it caused disruption of both intraparietal tracts passing through the inferior parietal lobule (e.g., tracts connecting the angular, supramarginal, postcentral gyri, and the superior parietal lobule) and fronto-parietal long tracts (e.g., the superior longitudinal fasciculus). The lesion site appears to be located more superiorly as compared to the cerebral regions shown active by other studies during tasks impaired in the syndrome, and it reached the subcortical area potentially critical in the emergence of the syndrome, as hypothesised in previous studies. Importantly, the reconstruction of tracts connecting regions within the parietal lobe indicates that this critical subcortical area is mainly crossed by white matter tracts connecting the angular gyrus and the superior parietal lobule. Taken together, these findings suggest that this case study might be considered as

* *Corresponding author*. University of Padova - Department of General Psychology (DPG), via Venezia 8, 35131 Padova, Italy.
E-mail address: mariagrazia.ranzini@unipd.it (M. Ranzini).
[1] These authors contributed equally to this work.
[2] These authors contributed equally to this work.
https://doi.org/10.1016/j.cortex.2023.05.016

empirical evidence of Gerstmann's tetrad caused by disconnection of intraparietal white matter tracts.

1. Introduction

Within the variety of impairments resulting from parietal lobe damage (Berlucchi & Vallar, 2018; Goodale & Milner, 1992), Gerstmann's syndrome (GS) has been consistently reported. GS is characterised by the common presence of acalculia, agraphia, finger agnosia and deficit in left/right orientation (Rusconi, 2018). Whether GS is caused by lesions in juxtaposed highly specialised brain areas, or whether it is due to disconnection between functionally relevant sub-regions, is a long lasting matter of debate (Ardila, 2020; Kleinschmidt & Rusconi, 2011).

GS was named after the neurologist Josef Gerstmann, who in 1924 described the case of a stroke patient presenting symptoms of finger agnosia, acalculia, left/right orientation problems, and agraphia, in absence of any language impairment (Gerstmann, 1924; for translation to English of the original article, see Rusconi & Cubelli, 2019). In 1927 Gerstmann reported two cases showing the same tetrad of symptoms, albeit these patients presented also other symptoms such as constructional apraxia, colour anomia and impaired number reading (Gerstmann, 1927, reviewed in Rusconi, Pinel, Dehaene, & Kleinschmidt, 2010). Similar cases were described in the same years by Herrmann and Pötzl (1926) and by Gerstmann himself (1930), and additional case reports were provided in the successive years and decades (for reviews see: Ardila, 2020; Basagni et al., 2021; Rusconi, Pinel, Dehaene, & Kleinschmidt, 2010). This syndrome received particular attention in view of the possibility to define a functional node within cognition-related brain networks (see: Rusconi et al., 2010). The main hypothesis was that this common cognitive node was most probably related to a culturally defined association between calculation and finger knowledge, albeit other accounts have been proposed (e.g., semantic processing; visuospatial mechanisms; etc.; see Rusconi et al., 2010). A developmental variant of GS has also been described (Kinsbourne & Warrington, 1963), further suggesting a critical role of hand-related processing in the development of numerical abilities (Rourke & Conway, 1997). The original Gerstmann's case and following case studies have suggested that the lesion in this syndrome is located in the parietal lobe, and, specifically, nearby the left angular gyrus (Gerstmann, 1924).

The idea of functional nodes within the parietal lobes has received attention, especially considering the involvement of the parietal lobes in multisensory integration, involving cognitive functions such as spatial cognition, working memory, calculation, action planning (e.g., Berlucchi & Vallar, 2018; Goodale & Milner, 1992; see also Ranzini et al., 2022). Nevertheless, there is no consensus on the existence of a functional node responsible for the GS symptoms, and a heated debate has characterised the most part of studies on GS (see Rusconi et al., 2010, for an historical perspective to this topic). Criticism originates from the fact that most of the existent GS case reports show additional symptoms (Benton, 1992), and pure GS has been barely reported (Rusconi, 2018). Symptoms which have been associated with the GS concern different forms of aphasia (e.g., Ardila, Concha, & Rosselli, 2000; Heimburger, Demyer, & Reitan, 1964; Poeck & Orgass, 1966; Sheimo, Bardach, & Hilfinger, 1997), in particular anomia (e.g., Gerstmann, 1927; Patil & Kulkarni, 2019), constructional apraxia (e.g., Mazzoni, Pardossi, Cantini, Giorgetti, & Arena, 1990; Moro, Pernigo, Urgesi, Zapparoli, & Aglioti, 2009; Stengel, 1944; Strub & Geschwind, 1974), hemianopia (e.g., Basagni et al., 2021; Gerstmann, 1924; Gerstmann, 1927; Herrmann & Pötzl, 1926), and autotopagnosia (e.g., Basagni et al., 2021; Carota, Di Pietro, Ptak, Poglia, & Schnider, 2004). Importantly, the four symptoms constituting GS can be found independently of each other (Heimburger, et al., 1964), further contrasting the idea of a cognitive mechanism common to all the four abilities impaired in GS.

Again, at the neuroanatomical level, brain regions other than the left angular gyrus have been also associated to GS, such as the left inferior frontal gyrus (Jõao, Filgueiras, Mussi, & Barros, 2017; Tanabe et al., 2020). The hemispheric lateralisation of the GS locus has been also questioned by a substantial number of GS cases showing impairment in the right hemisphere. For instance, Heimburger et al. (1964) found that, in a group of 111 neurological patients, 9% of patients had exclusively a damage in the right hemisphere, while in 13% of these patients brain damage was bilaterally distributed. Other cases of GS following damage in the right hemisphere have been reported (Hayashi et al., 2013; Moro et al., 2009; Sauguet, Benton, & Hecaen, 1971). Last but not least, the heterogeneity of testing does not permit precise estimates of the frequency of GS (Rusconi, 2018). All these factors led to consensus in considering GS an infrequent syndrome (Ardila, 2020), as well as to criticism regarding its classic interpretation as due to a common functional node across different cognitive functions.

An alternative account concerns the interpretation of GS as a disconnection syndrome (Kleinschmidt & Rusconi, 2011; Rusconi et al., 2009). Rusconi et al. (2009) conducted a functional magnetic resonance imaging (fMRI) study to investigate the neural substrate and pattern of white matter connections of the four abilities impaired in GS. In their study, healthy adults performed tasks involving number processing, left/right orientation, finger recognition, and writing. They found that these tasks activate specific subparts of the left inferior parietal lobe, with however no evidence of overlap between these areas. Crucially, they recorded and analysed diffusion tensor imaging (DTI) data in the same participants, and they found that subcortical fibres adjacent to the activated areas were connected to the neural areas active during the

execution of the four tasks. The authors provided specific—albeit tentative—indications concerning the locus of these subparietal fibres, through estimation of brain coordinates within regions of white matter with maximal interindividual reliability. They concluded that GS should arise from disconnection of intra-parietal subcortical tracts (see also Kleinschmidt & Rusconi, 2011).

Following the Rusconi and colleagues' hypothesis, however, only few studies have directly investigated the pattern of white matter disconnections underlying GS. Two recent single case studies found results in line with the disconnection revealed using the DTI technique. Specifically, in a recent study, Basagni et al. (2021) recorded DTI in a GS patient and reconstructed both large-scale fronto-parietal connections, and short intra-parietal subcortical tracts, in the left—lesioned—and right—preserved—hemisphere. They found that subcortical tracts connecting angular gyrus (AG), supramarginal gyrus (SMG), intraparietal sulcus (IPS), and post central gyrus (PCG) were completely damaged in the lesioned left hemisphere. Also, the left superior longitudinal fasciculus (SFL) was partially affected as compared to the right one. Another recent study by Papadopoulos et al. (2021) provided converging evidence, reporting DTI results in a GS patient indicating that both the SLF and parietal U-fibres were disconnected in the lesioned hemisphere as compared to the right hemisphere. Taken together, these two case reports provide important insights on the pattern of disconnections involved in GS, underlining the importance of single case studies in the understanding of the neuroanatomical correlates of rare syndromes.

To substantially contribute to this issue, we report here the results of a detailed neuropsychological and neuroanatomical investigation of a patient presenting the four GS symptoms. During the stay in the Hospital, the patient received an extensive neuropsychological assessment, and was enrolled in research protocols. GS was assessed by means of batteries and tasks for number processing, fingers knowledge, left/right orientation, and writing. The patient also presented optic ataxia. Optic ataxia consists in the difficulty to reach a target with the arm, independently of any other visual, cognitive, or motor impairment (Rossetti, Pisella, & McIntosh, 2019). In our patient, optic ataxia was assessed across many trials and sessions where the patient was asked to reach and grasp an object in peripheral vision. Finally, the patient showed difficulties also in processing ordinal time sequences (e.g., days of the week, months of the year). The patient did not present signs of aphasia nor of autotopagnosia. We investigated the neuroanatomical correlates of the patient's impairment through lesion mapping, atlas-based estimation of probability of white matter tracts disconnection, and DTI-based tractography. Crucially, the brain lesion in this patient was of interest because it was located more superiorly in the left parietal lobe as compared to the traditional locus of GS, and it was at the border of the tentative location indicated by Rusconi et al. (2009). We reconstructed from the DTI data: first, the subcortical fibres at the whole-brain level crossing through the tentative location indicated by Rusconi et al. (2009) to describe to which extent a lesion in this location causes disconnection of areas close and far from the lesion; second, the atlas-based parietal tracts (Catani et al., 2017) to describe the amount of damage of each tract in the left lesioned hemisphere as compared to the right healthy hemisphere; third, the specific parietal tracts which cross the location indicated by Rusconi et al. (2009) to provide indications about the belonging of this area to each tract. The extensive neuroanatomical and neuropsychological investigation allowed a ground-breaking direct test of the Rusconi's et al. hypothesis.

2. Case report

The patient was a 51-years old right-handed woman with 8 years of education who arrived at the IRCCS San Camillo Hospital and was examined two months after a haemorrhagic stroke. At hospitalisation, MRI highlighted a left parieto-occipital lesion. The brain lesion was located in the left SPL in and around the intraparietal sulcus. The patient's speech was informative and fluent, the patient had a good awareness relative to her difficulties and was particularly compliant with the assessment. The performance at the motor assessment evaluating the upper limb reach-to-grasp movement, quality and compensatory movements, was at ceiling (36/36 at the Reaching Performance Scale: RPS, Levin, Desrosiers, Beauchemin, Bergeron, & Rochette, 2004). Nonetheless, a motor deficit concerning strength and coordination impairments of the contralesional upper limb were qualitatively observed by the physiotherapists, and these impairments were under treatment during hospitalisation. The neurological assessment excluded any sign of oral language deficit, that is, production, repetition, and comprehension were within the norms. The patient underwent a full neuropsychological assessment conducted by expert neuropsychologists in 5 consecutive meetings in the subchronic period following the cerebro-vascular accident (2 months from stroke). The neuropsychological assessment included the following tests: Mini Mental State Examination (MMSE) (Magni, Binetti, Bianchetti, Rozzini, & Trabucchi, 1996), Montreal Cognitive Assessment (MoCA) (Santangelo et al., 2015), Frontal Assessment Battery (FAB) (Appollonio et al., 2005), Raven Coloured Progressive Matrices (CPM) (Raven & Court, 1990), Stroop test (Caffarra, Vezzadini, Dieci, Zonato, & Venneri, 2002a), Trail Making Test (TMTa and TMTb) (Giovagnoli et al., 1996), semantic and phonemic fluency (Novelli, Papagno, Capitani, & Laiacona, 1986), backward and forward digit span (Monaco, Costa, Caltagirone, & Carlesimo, 2013), forward spatial span (Spinnler e Tognoni 1987), Rey Complex Figure (Caffarra, Vezzadini, Dieci, Zonato, & Venneri, 2002b), Rey Auditory Verbal Learning Test (RAVLT) (Carlesimo, et al., 1996), Benton Test (Benton, Varney, & Hamsher, 1983), Visual Object Recognition Test (Warrington & James, 1991), Modified Five Point Test (MCST) (Cattelani, Dal Sasso, Corsini, & Posteraro, 2011), Modified Card Sorting Test (MCST) (Caffarra Vezzadini, Dieci, Zonato & Venneri, 2004), De Renzi's test for apraxia (De Renzi, Pieczuro, & Vignolo, 1968). The results from this neuropsychological assessment are reported in Table 1. The patient was mainly impaired at the level of executive functioning, visuospatial processing, and object recognition. The impairment in semantic fluency in our patient was most likely due to the executive component of the task, as well as to difficulties related to access to lexicon and

Table 1 – The patient's raw (RS) and corrected (CS) scores at the first evaluation. Cut-off values indicate the score above/below which the performance is to be considered in the normality range. Score ranges of each test, where applicable, are also provided.

Cognitive domain	Neuropsychological test	RS	CS	Cut-off (range)
General cognitive functioning	Montreal Cognitive Assessment (MoCA)	17	18	≥15.5 (0–30)
	Mini Mental State Examination (MMSE)	**23**	**22.97**	≥24 (0–30)
Attention and Executive functions	Frontal Assessment Battery (FAB)	**13**	**12.99**	≥13.4 (0–18)
Attention and Executive functions – visual search	Attentive Matrices	**8**	**7**	≥23.9 (0–50)
	Trail making test- A	95	85	≤94
Attention and Executive functions – alternate attention	Trail making test- B	**402**	**365**	≤283
Attention and Executive functions – shifting	Trail making test B-A	**307**	**208**	≤187
Attention and Executive functions – response inhibition	Stroop Test			
	Time	**48.5**	**48**	≤36.92
	Errors	0	0	≤4.24
Attention and Executive functions – working memory	Backward digit span	3	3.02	>2.65 (0–8)
Attention and Executive functions – flexibility	Phonemic fluency	**15**	**17**	≥17.35
	Modified Card Sorting Test (MCST)			
	Number of categories	6	6	≥2 (0–6)
	Perseverative errors	1	1	≤6.41
	Modified five points test			
	Unique drawings	**12**	**17.75**	≥23.84
	Errors	1	7.69	≤22.46
Language	Designation on description	35	35	≥33.25 (0–38)
	Semantic fluency	**22**	**23**	≥24
Memory – verbal short term	Forward digit span	6	6.04	>4.26 (0–9)
Memory – spatial short term	Spatial span	**3**	**2.99**	≥3.25 (0–9)
Memory – spatial learning	Spatial Supraspan	24.83	21.08	≥1
Memory	Rey Auditory Verbal Learning Test			
Verbal learning	*Immediate recall*	**27**	**26.2**	≥28.53 (0–75)
Verbal long term	*Delayed recall*	**5**	**4.6**	≥4.69 (0–15)
Non-verbal intelligence	Raven Coloured Progressive Matrices	31	31.3	≥18.96 (0–36)
Visuospatial abilities	Rey complex figure			
Visuospatial construction	*Copy*	**24**	**24.25**	≥28.87 (0–36)
Spatial long term memory	*Recall*	20	21.5	≥9.46 (0–36)
Visuospatial abilities	VOSP Objects			
	Incomplete letters	20		>16 (0–20)
	Silhouettes	23		>15 (0–30)
	Objects decision	**8**		>14 (0–20)
	Progressive silhouettes	**9**		>15 (0–20)
	VOSP spatial			
	Points count	**8**		>8 (0–10)
	Position discrimination	20		>18 (0–20)
	Numbers position	8		>7 (0–10)
	Cube analysis	8		>6 (0–10)
Apraxia	De Renzi test for apraxia			
	Imitation of gestures			
	Right hand cumulative scores	64		≥53 (0–72)
	Left hand cumulative scores	68		≥53 (0–72)
	Gestures on command			
	Right hand cumulative scores			≥18 (0–48)
	Meaningful gestures	10		
	Use of objects	10		
	Left hand cumulative scores			≥18 (0–48)
	Meaningful gestures	11		
	Use of objects	11		
	Orofacial apraxia	18		≥16 (0–20)

semantic storage, general slowness, and pre-morbid low level of formal education.

Additional testing revealed that the patient also presented with severe optic ataxia. The test for the diagnosis of optic ataxia consisted of a shorter version of the standardised test by Borchers and colleagues (Borchers, Müller, Synofzik, & Himmelbach, 2013), originally proposed by Perenin and Vighetto (1988). The patient was asked to reach and grasp a wooden stick presented on her left or right side, while looking at a central fixation point (a camera's lens). At each trial, the stick was shown by the experimenter, which stood behind the patient. Stick size, position, instructions and procedure were the same as in Borches and co-workers (2013), except for the number of trials. Specifically, the patient carried out a total of 20 trials, 5 with the ipsilesional hand in the ipsilesional hemifield, 5 with the ipsilesional hand in the contralesional

hemifield, 5 with the contralesional hand in the contralesional hemifield, and finally 5 with the contralesional hand in the ipsilesional hemifield. Considering that a complete segregation of ventral and dorsal streams has been questioned by several studies (Pisella et al., 2009; Budisavljevic, Dell'Acqua, & Castiello, 2018; Sim et al., 2015), the impairment in object recognition in our patient was more likely due to optic ataxia.

Following a first evaluation, the patient underwent a cognitive rehabilitation protocol by means of a digital tool combining prismatic adaptation with cognitive exercises (Giustiniani et al., 2022). Specifically, the rehabilitation protocol included 10 sessions (5 sessions/week) of prismatic adaptation combined with computerized cognitive tasks. Prismatic adaptation included a digital pointing task in which a black square was randomly presented on the white screen of a tablet in three possible positions: central, right or left part of the screen. The patient was asked to point to the square with the right hand. The pointing task was performed in three conditions: pre-exposure (30 trials), exposure (90 trials), post-exposure (30 trials). In the exposure condition, the patient performed the pointing task while wearing prims inducing a 10° shift of the visual field to the left visual field (accordingly with the patient's lesion side). The pointing task was followed by computerized cognitive tasks performed on a tablet to train attention, executive functions, visuospatial abilities, and calculation.

After the beginning of the rehabilitation protocol, the patient underwent a second evaluation with the same test for optic ataxia. At the first evaluation, the patient presented severe bilateral crossed optic ataxia (100% errors with the right–contralesional–hand, when the object was presented either on the left or the right side). The performance with the left hand was preserved but not free of errors (20% errors when the object was presented on the left side, and 0% errors when the object was on the right). At the second evaluation, the patient showed a certain degree of improvement in the performance, with 0% errors with the left hand in both the left and right object conditions, and 20% errors with the right hand and the object on the left. The performance with the right hand and the object on the right remained however severe (100% errors). A new cognitive assessment was extensively conducted at the end of the rehabilitation protocol. The effects of rehabilitation are outside the scope of this paper, and they are described elsewhere (see: Giustiniani et al., 2022), so we report here the results of the first two evaluations.

Mild signs of apraxia were also detected during experimental testing, with occasional slow and imprecise movements when required to pantomime the use of everyday objects, or to imitate meaningful or meaningless gestures (the testing procedure was adapted from Tessari, Toraldo, Lunardelli, Zadini, & Rumiati, 2015). These findings were however not confirmed at the clinical examination (see Table 1). Finally, the patient showed consistent difficulties when dealing with temporal sequences, namely when required to indicate the day of the week preceding or following a reference (e.g., the day of the week preceding Saturday; 4/14 errors), or to indicate the month of the year preceding or following a reference (e.g., the month of the year following June; 4/10 errors).

Overall, the observed cognitive impairment was compatible with the severity of the clinical condition and the lesion site of the patient. Specifically, the neuropsychological assessment mainly revealed impairment of a spatial nature. Importantly, the patient exhibited good and fast recovery since the beginning of hospitalisation, being compliant and highly motivated. The presence of GS was then assessed by specific testing to assess calculation, fingers agnosia, left/right orientation problems, and agraphia. These tests and the resulting patient's performance are described below (Section 2.1). This case report is part of the study approved by the Ethics Committee of Venice and IRCCS San Camillo Hospital (Venice, Italy), reference number 2020.04. We report all data exclusions (if any), all data inclusion/exclusion criteria, whether inclusion/exclusion criteria were established prior to data analysis, all manipulations, and all measures in the study. Written informed consent was obtained from the patient. No part of the study procedures or analysis plans was pre-registered prior to the research being conducted. The data are contained in the manuscript. The integral original MRI scan and DTI data cannot be publicly available because they are ethically sensitive content, and they are therefore subject to ethical restrictions. Ethically sensitive content is contained also in the analysis code and is therefore subject to ethical restrictions. We do not have legal permission to publicly archive the materials used in this study. Readers seeking access to the materials should contact the owner: Francesca Burgio francesca.burgio@hsancamillo.it.

2.1. *Assessment of Gerstmann's syndrome*

The presence of GS symptoms was assessed throughout a series of batteries and tasks indicating the presence of signs of acalculia, finger agnosia, left/right orientation problems, and agraphia.

2.1.1. *Acalculia*

The Numerical Activities of Daily Living–Short (NADL–short form; Burgio et al., 2022) was administered to the patient to assess numerical competence. The test was specifically designed to assess formal and informal numerical difficulties in neurological patients with heterogeneous diagnoses. It is composed of two main parts: the Informal Test, investigating patient performance in daily tasks involving numbers (time, measurement, transportation, communication, general knowledge, money); the Formal Test assessing scholastic skills into 5 sub-sections.

- Number comprehension (maximum score = 3), in which the patient is required to point to the digit equivalent to the number of squares showed in a panel;
- Transcoding abilities (maximum score = 6), in which the patient is required to read out loud written digits or write down numbers presented orally;
- Mental calculation (maximum score = 3), requiring the patient to perform mental multiplications;
- Arithmetics rules and principles (maximum score = 6), in which the patient is asked to solve some operations using basic principles (e.g., commutativity principle);

- Written operations (maximum score = 6), in which the patient is required to perform and report the result of subtractions and multiplications.

The patient's performance was corrected according to the normative data (Burgio et al., 2022). The patient obtained a normal performance in the NADL–short form Informal test (score 19/23) and in all the sub-sections of NADL–short form Formal test, except in the written operations (score 2/6), exhibiting a focal deficit in calculating multiplications. This aspect was confirmed by a further test employed to assess calculation, i.e., the "*Batteria di test per l'acalculia*" (Miceli & e Capasso, 1991). This battery allows the evaluation of several domains concerning numerical abilities (e.g., transcoding, numerical judgments, mental and written calculation). Given that a comprehensive evaluation of numerical abilities has been performed using the NADL–short form battery, only the written operation sections of the Miceli's battery was administered to the patient, in which she performed within the normal range in calculating both additions (score 20/20) and subtraction (score 17/20), whereas she showed several difficulties in executing multiplications (score 7/20). In particular, in multiplication, the patient exhibited difficulties in recalling both the multiplication facts and the correct alignment of numbers in the columns, especially for multiplications with more than 2 digits. Thus, the calculation resulted in number position errors and in incorrect calculation.

Difficulties in number processing were also observed when the patient was required to compare digits magnitude (e.g., "*Is 4 larger or smaller than 5?*": 11% errors on 36 trials), when required to give a number smaller or larger than a reference (e.g., "*Could you give me a number larger than 142?*"; 25% of errors on 12 trials), and when she was asked to perform number interval bisection (e.g., "*What is the mid-number between 13 and 19?*", adapted from Zorzi, Priftis, & Umiltà, 2002, p. 78% errors on 18 trials).

2.1.2. *Finger agnosia*

The presence of finger agnosia was fully explored by means of finger recognition and finger naming tasks. The tests were administered in separate sessions. The adopted procedure is fully described in previous works (Moro et al., 2009; D'Imperio, Tomelleri, Moretto, & Moro, 2017). Finger recognition was carried out with three types of instructions (verbal, visual or tactile) and two response modes (verbal or pointing), in order to control influences of primary processes. The test was administered in separate blocks of 25 items according to the characteristics of instructions and responses. The instructions required recognition of one finger at a time, prompted by name spoken by the examiner (i.e., verbal), by visual indication on the patient's hand or template (i.e., visual) or by touch on the patient's hand (i.e, tactile). The responses were requested by oral naming (i.e., verbal) or by pointing to the patient's own hand or silhouette of a hand (i.e., pointing). The test was repeated for the right hand and the left hand in order to check for hand-specific deficits. Two additional control tasks are performed. A first task asked to name the fingers of the hand on semantic description (with 10 items), in order to rule out vocabulary access problems. A second task of body part recognition on verbal instruction and response by pointing (with blocks of 18 items based on response characteristics), to control for generalised deficits. The patients showed impairment particularly with verbal instruction and tactile stimulation, in absence of general autotopagnosia (see Table 2). Additionally, when asked to verbally indicate the correct fingers for meaningful gestures (e.g., calling, to point, the ring finger) she occasionally failed (1/6 errors). The presence of finger agnosia was also suggested by the patient's performance at ten following trials of finger recognition and finger naming tasks: the patient was very slow and felt insecure when reporting finger after touch on the right hand, in absence of deficit in naming fingers on a hand image.

2.1.3. *Left/right orientation problems*

The assessment for left/right orientation problems was based on questions on recognition of left/right parts of one's body or on requests to point parts of one's body in the mirror or on the experimenter's body. The patient's performance was very slow and overall impaired in both types of tasks (8/10 correct when pointing to body parts directly, and 1/4 correct when pointing to body parts through the mirror). The presence of left/right orientation problems was also confirmed by the patient's performance at an experimental additional test: the patient could not correctly point toward the experimenter's body parts (right shoulder and right hand) upon request (2/3 errors).

2.1.4. *Agraphia*

Three types of agraphia have been previously described in the context of GS: 1) aphasic agraphia characterised by the presence of omissions and substitutions but with preserved form of the letters; 2) apraxic agraphia, in which letters have incorrect form; 3) spatial agraphia consisting in defective management of space on the sheet (Roeltgen & Heilman, 1985). The patient's deficit can be ascribed to all the three types of agraphia. Additionally, she complained about her difficulties in remembering specific rules of the Italian language such as the use of accents and apostrophes and how to use the third person of the present indicative tense of the verb "*to be*", or the ability to distinguish the "*o*" used as a conjunction ("or" in English) from the "*ho*" relative to the first person of the present indicative of the verb "*to have*". Agraphia was tested by asking the patient to write the alphabet (upper and lower cases), to write her name, to copy and to write simple spontaneous or under dictation sentences. Additionally, the patient was asked to write some higher -level sentences requiring a good formal knowledge of the Italian language. In this task, the patient's writing was uncertain and extremely slow, requiring a long time to recall syntactic rules and complete the sentences. She needed continuous feedback with respect to the correctness of the sentences and she asked to have the chance to correct for errors during her writing. The presence of agraphia was confirmed by grammar errors in both writing under dictation and in spontaneous writing, as well as by the presence of omissions of letters or typefaces (see Table 3). Additionally, a wrong management of space on the sheet was present, with writing not respecting the horizontality or the margin of the paper.

Table 2 – Results from the main assessment for autotopagnosia and finger agnosia (Moro et al., 2009; D'Imperio et al., 2017).

Deficit	Test	Response Modality	Score
Autotopagnosia	Body's parts identification - verbal instructions	*Pointing to own body with closed eyes*	18/18
		Pointing to own body with open eyes	18/18
		Pointing to experimenter's body	18/18
		Pointing to human figure (silhouette)	18/18
Finger Agnosia	Finger identification -verbal instructions	*Pointing to own right hand*	18/25
		Pointing to own left hand	14/25
	Finger identification -visual instructions on patient's hand	*Verbal answer and own right hand*	24/25
		Verbal answer and own left hand	24/25
		Verbal answer and pointing to the silhouette of a right hand	19/25
		Verbal answer and pointing to the silhouette of a left hand	22/25
	Finger identification -visual instructions on experimenter's hand	*Pointing to right hand*	25/25
		Pointing to left hand	23/25
	Finger identification -visual instructions on the silhouette	*Pointing to right hand*	25/25
		Pointing to left hand	24/25
	Finger identification -Tactile instructions on the silhouette	*Verbal answer/right hand*	25/25
		Verbal answer/left hand	23/25

2.2. Neuroanatomical investigation

Neuroimaging acquisitions were performed on a 3T Philips Ingenia scanner (32-channel receiver head coil) at Hospital San Camillo IRCCS. The acquisition protocol consisted of anatomical scan and DTI scan acquired 4 months after stroke. Details are reported in the next sections.

2.2.1. Lesion mapping

The patient underwent an anatomical MRI scan at the Hospital. The anatomical scan consisted of a 3-dimensional Magnetization Prepared T1 weighted (T1w) Rapid Acquisition Gradient Echo (MPRAGE) sequence acquired at 0.8 mm isotropic resolution, flip angle = 8°, repetition/echo/inversion times TR/TE/TI = 9.8/4.5/950 ms, field of view (FOV) = 250 × 250 × 200 mm^3, SENSE acceleration 2 and 2.6 along primary (Anterior-Posterior (AP)) and secondary (Right/Left (RL)) phase encoding directions. Total scan time was 5 min and 25 s. The patient's lesion was mapped by means of a semi-automated procedure, consisting of mapping the lesion with *Clusterize* (de Haan, Clas, Juenger, Wilke, & Karnath, 2015), an algorithm which automatically delineates the lesion while also allowing to manually check and correct the output. We used MRIcron software (https://people.cas.sc.edu/rorden/mricro/mricro.html, Rorden, 2019) for lesion visualisation and final mask correction. This step was performed independently by two authors (MR and DD), and a common version of lesion mapping was obtained through consensus. Finally, the lesion map was checked by a neuroradiologist (VD). The patient's lesion (in anatomical space) is graphically represented in Fig. 1a. The lesion mask and the patient's brain image were registered to the standard MNI152 template and projected onto the MNI space by means of diffeomorphic non-linear transformation which accounted the presence of the lesion, implemented in the BCBtoolkit software (http://toolkit.bcblsb.com, Foulon et al., 2018).

This lesion mapping procedure overall confirmed the clinical report. The lesion was located entirely in the left hemisphere. Overlap between the lesion and the Automated Anatomical Labelling template (Rolls, Joliot, & Tzourio-Mazoyer, 2015) indicated that the lesion centre of mass was located in the left superior parietal lobule (MNI coordinates: −23,-55,45; 62% of damage within this area), extending anteriorly to the left postcentral gyrus (12% of damage), posteriorly to the left middle and superior occipital gyri (5% and 29% of damage, respectively), and inferiorly to the left inferior parietal lobule (18% of damage) reaching the angular gyrus (2% of damage). Medially, the lesion involved the left cuneus and precuneus (11% and 12% of damage, respectively).

2.2.2. Atlas-based estimation of probability of disconnection

The normalised brain images and lesion mask were used to extract probability of white matter tracts disconnection through comparison against tracts atlases. The method was validated by previous works (e.g., Foulon et al., 2018), implemented in the BCB toolkit, and currently in use for investigation of white matter tracts disconnection following neurological damage (e.g., Dulyan et al., 2022; Pacella et al., 2020). Following previous studies (Foulon et al., 2018), only probabilities larger than 50% were considered as indexes of

Table 3 – Examples of sentences wrote by the patient under dictation. The patient wrote only 3 sentences out of 9 without spelling or grammatical errors. Errors are highlighted in italic.

Correct sentence (under dictation)	Sentence wrote by the patient
Non c'è né se né ma che tenga	Non c'è *ne* se *ne* ma che tenga
Ho comprato un libro nuovo	*O* comprato un libro nuovo
Sono indeciso tra due gusti di gelato	Sono indeciso *trai* due gusti di gelato
O fragola *o* banana	O fragola *o* banana
Oggi è lunedì	Oggi *siamo* lunedi
Domani viene a trovarmi mio figlio	Domani viene a trovarmi mio figlio
Sono già passati tre mesi dal mio ricovero	Sono già passati *3* mesi *da* mio ricovero
Se riesco oggi vado al mare a fare una passeggiata	Se riesco oggi vado al mare a fare una *passegiat*
Vorrei tanto ritornare alla mia vita di prima	Vorrei tanto ritornare alla mia vita di prima

white matter tracts disconnection. A large probability of disconnection was found at the level of the left superior longitudinal fasciculus I (100%), left superior longitudinal fasciculus II (100%), the corpus callosum (100%), and the left cingulum (100%). Disconnection was highly probable also at the level of the long segment of the arcuate fasciculus (60%), left hand superior U-tract (86%), left inferior fronto-occipital fasciculus (88%), left inferior longitudinal fasciculus (84%), the anterior commissure (80%), and the left superior longitudinal fasciculus III (58%). The disconnectome map allows clarifying the extent and location of disconnection, and it is represented in Fig. 1b. All the brain regions affected by the lesion within the left hemisphere resulted as disconnected (i.e., superior and inferior parietal lobuli, angular gyrus, postcentral gyrus, occipital gyrus, cuneus, and precuneus). The disconnection reached anteriorly the frontal middle and superior gyri, inferiorly the middle temporal gyrus, the insula and parahippocampal area, the basal ganglia (mainly putamen and thalamus), as well as the cingulum within the left and right hemispheres.

2.2.3. *DTI-based tractography*

Multi b-value DTI data were acquired using an in-plane isotropic resolution and a slice thickness of 2.2 mm and 2.4 mm, respectively. An in-plane SENSE factor of 2 was employed. The phase encoding direction was set to be AP. Sixty slices were acquired with a multiband factor of 3. FOV was $220 \times 220 \times 144$ mm^3 3 b-values (700, 2000 and 3000 s/mm^2) each with 32 directions and one b0 image were acquired. Flip angle and refocusing angles were 90°/180°, TE = 109 ms and TR = 2800 ms. Total scan time was 4 min and 38 s. To correct for susceptibility-induced spatial distortions, an EPI sequence with opposite phase encoding direction with no diffusion weighting was acquired using the same TR/TE combination and readout settings.

The MRTricks3 software (Tournier et al., 2019) was employed to pre-process the DTI data and to perform tractography. In particular, the DTI data were firstly denoised according to the procedure described in Veraart et al. (2016). Then, distortion (Andersson, Skare, & Ashburner, 2003), eddy currents and motion (Andersson & Sotiropoulos, 2016) correction was applied. To resolve for crossing fibres, constrained spherical deconvolution (CSD) was employed (Tournier et al., 2008). Specifically, fibre density distributions (FODs) of white matter, together with grey matter plus CSF tissue compartments were estimated. Finally, to constrain the tractography algorithm using anatomical priors, a five-tissue-type (5 TT) segmentation (Smith, Tournier, Calamante, & Connelly, 2012) was computed from the anatomical T1w data. Note that the last layer of the segmentation corresponded to the lesion mask in individual space described in Section 2.2.1.

DTI data were used for tractography following two specific and independent aims: first, to reconstruct and evaluate the number of fibres passing through the locus indicated by Rusconi et al. (2009),[3] respectively on the left (i.e. the part of the brain containing the lesion) and on the right (i.e. the healthy part of the brain); second, to compare the left vs. the right white matter fibre bundles in the parietal lobes as described by Catani et al. (2017). To achieve the first aim, a seed for the tractography algorithm was drawn according to the following procedure. A 3D spherical mask (12 voxels diameter) centred on the seed coordinate was drawn using ITK-SNAP (http://www.itksnap.org/pmwiki/pmwiki.php, Yushkevich et al., 2006) in MNI space. A homologous spherical seed on the right hemisphere was drawn for comparison. The masks were projected to the DTI space using the inverse of the diffeomorphic transformation computed in Section 2.2.2. Interpolation was performed using the nearest neighbour followed by dilation and erosion operations. Tractography was performed on the left and on the right hemispheres, separately. This was done using the tckgen function of MRTricks3. Specifically, the algorithm employed the left/right masks in DTI space (1.000.000 seed positions chosen at random within the projected masks), the 5 TT segmentation to make full use of the anatomical priors, and the FODs as input. Note that, finally, the two runs of the algorithm were constrained so that streamlines could not enter the other hemisphere by masking out the corpus callosum.

To achieve the second aim, we performed the following steps. In order to reconstruct the parietal tracts described by Catani et al. (2017), we employed the AAL3 atlas (Rolls, Huang, Lin, Feng, & Joliot, 2020). By merging the information included within the AAL3 atlas and the individual tracts reported in Catani et al. (2017), we were able to identify a finite set of target

[3] Rusconi and colleagues reported two MNI brain coordinates (i.e., −35, −38, 35, and −35, −45, 33; Rusconi et al., 2009) resulting from the sum of the individual normalised fibre bundle overlap across brain regions active in the four investigated domains (number processing, left/right orientation, finger knowledge, and writing).

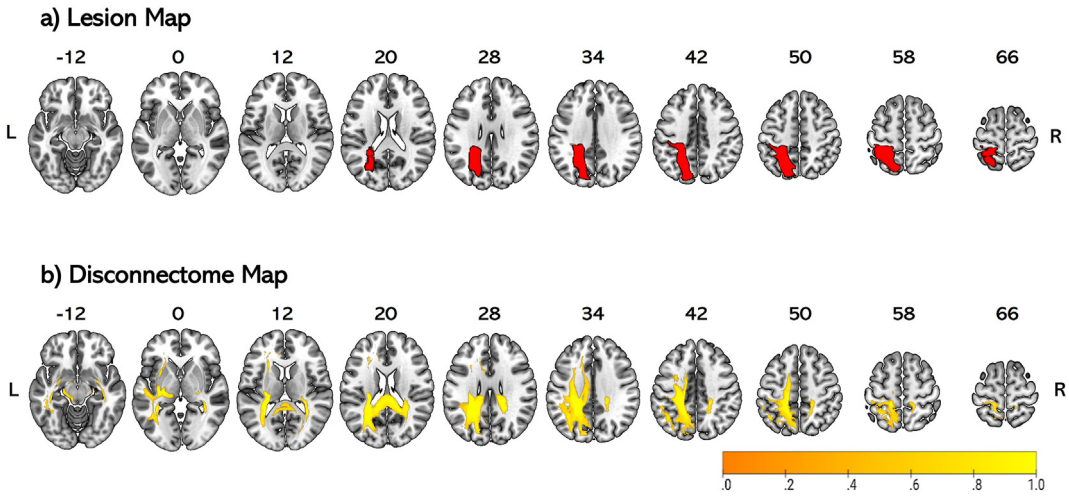

Fig. 1 – Panel a. The patient's standardised lesion on the MNI template. Panel b. The patient's disconnectome map is shown on the MNI template, and it represents the probability of disconnection at the voxel level (Foulon et al., 2018). Images obtained using MRIcroGL (https://www.nitrc.org/projects/mricrogl/, Rorden & Brett, 2000).

fibre bundles corresponding to the following tracts: the PAS (Parietal Angular-to-Supramarginal), connecting the angular and the supramarginal gyri; the PIST-AG (Parietal Inferior-to-Superior tract, Angular), connecting the angular gyrus and the superior parietal lobule; the PIST-SMG (Parietal Inferior-to-Superior tract, Supramarginal), connecting the supramarginal gyrus and the superior parietal lobule; the PIP-AG (Parietal Inferior-to-Postcentral tract, Angular), connecting the angular gyrus and the postcentral gyrus; the PIP-SMG (Parietal Inferior-to-Postcentral tract, Supramarginal), connecting the supramarginal gyrus and the postcentral gyrus; and the PSP (Parietal Superior-to-Postcentral), connecting the superior parietal lobule and the postcentral gyrus (Fig. 3a; see Catani et al., 2017, for a detailed explanation of individual tracts).

To perform tractography, the following steps were undertaken: after registering the atlas on the individual patient's MRI space using the inverse of the diffeomorphic transformation computed as part of our first submission, we included additional constrains (to the ones already described, i.e. 5 TT segmentation, number of seeds etc.) to the tractography algorithm: for each tract, we defined directly from the projected atlas its anatomical extremities (for example, when

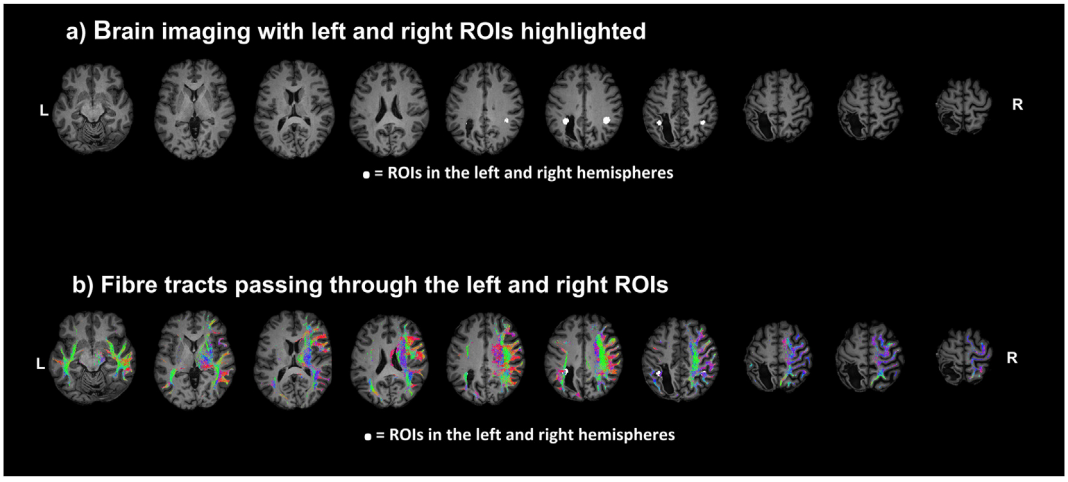

Fig. 2 – Panel a: The patient's brain images showing the lesion in the patient's MRI space. The ROIs are plotted in white, within the left and the right hemispheres. ROIs were drawn around the site defined by Rusconi et al. (2009) in the left hemisphere (MNI coordinate: −35, −41, 34) and around a homologous site in the right hemisphere (MNI coordinate: 35, −41, 34). This procedure is described in detail in Section 2.2.3. Panel b: Reconstruction of white matter crossing the defined ROIs within the left and right hemispheres (see Section 2.2.3 for details; see also Fig. 3b). Note that we masked the corpus callosum to allow a cross-hemispheric comparison. However, because of this masking procedure, streamlines across hemispheres were not tracked.

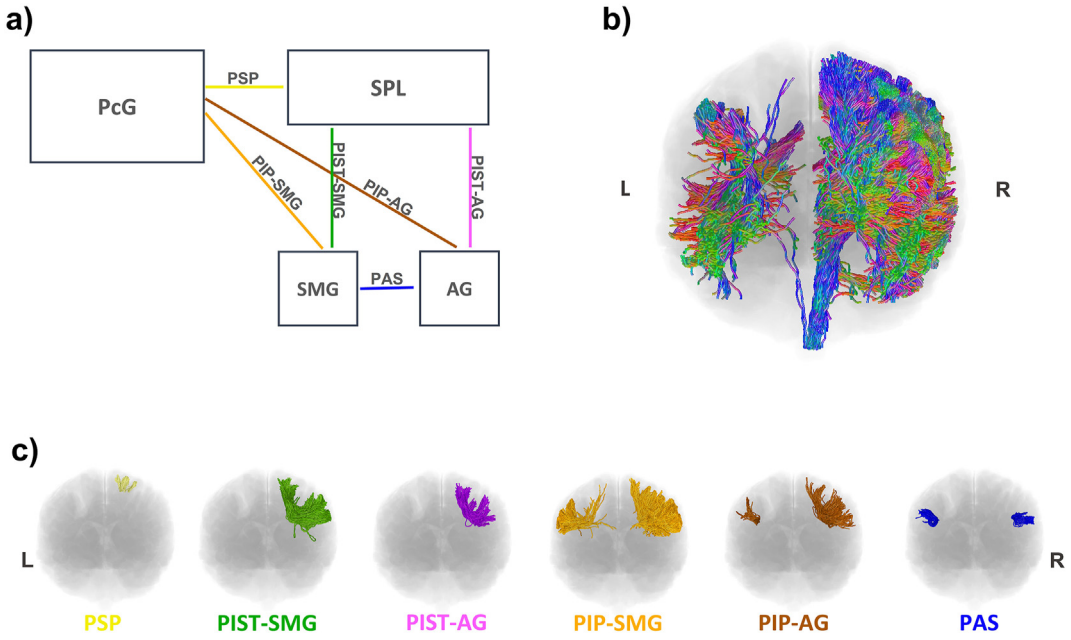

Fig. 3 – Panel a: schematic illustration of the brain areas and the parietal tracts that have been considered in tractography (PcG = Post–central gyrus; SPL = Superior Parietal Lobule; SMG = Supramarginal Gyrus; AG = Angular gyrus; PSP = Parietal Superior-to-Postcentral; PIST-SMG = Parietal Inferior-to-Superior Tract, Supramarginal; PIST-AG = Parietal Inferior-to-Superior Tract, Angular; PIP-SMG = Parietal Inferior-to-Postcentral, Supramarginal; PIP-AG= Parietal Inferior-to-Postcentral, Angular; PAS = Parietal Angular-to-Supramarginal). Panel b: Reconstruction of white matter crossing the defined ROIs within the left and right hemispheres (posterior view; see Section 2.2.3 for details; see also Fig. 2b). Panel c: 3D representation of PAS, PIST-AG, PIST-SMG, PIP-AG, PIP-SMG and PSP tracts. Note that in this illustration, fibres were not constrained to pass through the ROI indicated by Rusconi et al. (2009).

performing tractography of the PIP-AG, the Angular Gyrus and the Postcentral gyrus were retrieved from the atlas and used as masks through which streamlines had to either seed and/or pass through). Reconstructed tracts corresponded to those streamlines connecting the masks (predominantly through white matter tissue). Note that to enforce this last aspect, all cortical regions of the atlas other than the masks just defined (plus the inferior parietal lobule, since the majority of the target tracts pass through this region), were excluded (i.e, streamlines could not pass through it). Note that when this semi-automatic procedure failed, we provided additional exclusion masks which were drawn based upon track specific anatomical considerations. This happened for PAS, PIP-SMG, and PSP. For each tract we additionally computed the fractional anisotropy (FA). The method we adopted consisted in estimating the FA for each streamline, and then computing the mean FA and standard deviation (SD) of all the streamlines within each tract. Finally, to assess whether each of the considered tracts passed through the ROI drawn following Rusconi et al. (2009), the same analysis was repeated considering the ROI indicated by Rusconi et al. (2009) as a hub through which streamlines had to pass through.

The output of tractography is illustrated in Figs. 2–4. Critically, the seed region in the left hemisphere was located at the periphery of the patient's lesion (see Fig. 2a). Considering that cortical thinning around the lesion was visible in radiological images, it is reasonable to consider this region to be compromised. Remarkably, the reconstruction of fibres crossing the ROI indicated by Rusconi et al. (2009) at the whole brain level clearly shows the patient's degree of cerebral disconnection within the left hemisphere as compared to the right hemisphere (Figs. 2b and 3b): disconnection is mainly observed at the level of the dorsal stream and of intra-parietal connections (Figs. 2b and 3b, left hemisphere). Note that in this analysis the number of tracked fibres which satisfied all the tractography constraints was 34,703. In contrast, the number of tracked fibres which satisfied all the tractography constraints in the healthy hemisphere was 371,386, i.e., approximately ten fold increase as compared to the left lesioned hemisphere, resulting in the tracking of a dense network of fibre bundles across all lobes (Figs. 2b and 3b, right hemisphere).

Figs. 3c and 4 illustrate PAS, PIST-AG, PIST-SMG, PIP-AG, PIP-SMG, and PSP fibre bundles reconstructed without the ROI indicated by Rusconi et al. (2009) as constraint. Table 4 reports for each tract a comparison between the streamlines found in the left lesioned hemisphere as compared to the healthy right hemisphere when tractography was computed without considering the ROI defined following Rusconi et al. (2009). With this procedure, it was possible to track all bundles on the healthy side of the brain (right). However, PIST-AG, PIST-SMG, PSP did not exist on the left lesioned hemisphere (number of streamlines and FA (M and SD) in: left PIST-AG = 0; right PIST-AG = 438, FA M = .49, SD = .03; left PIST-SMG = 0;

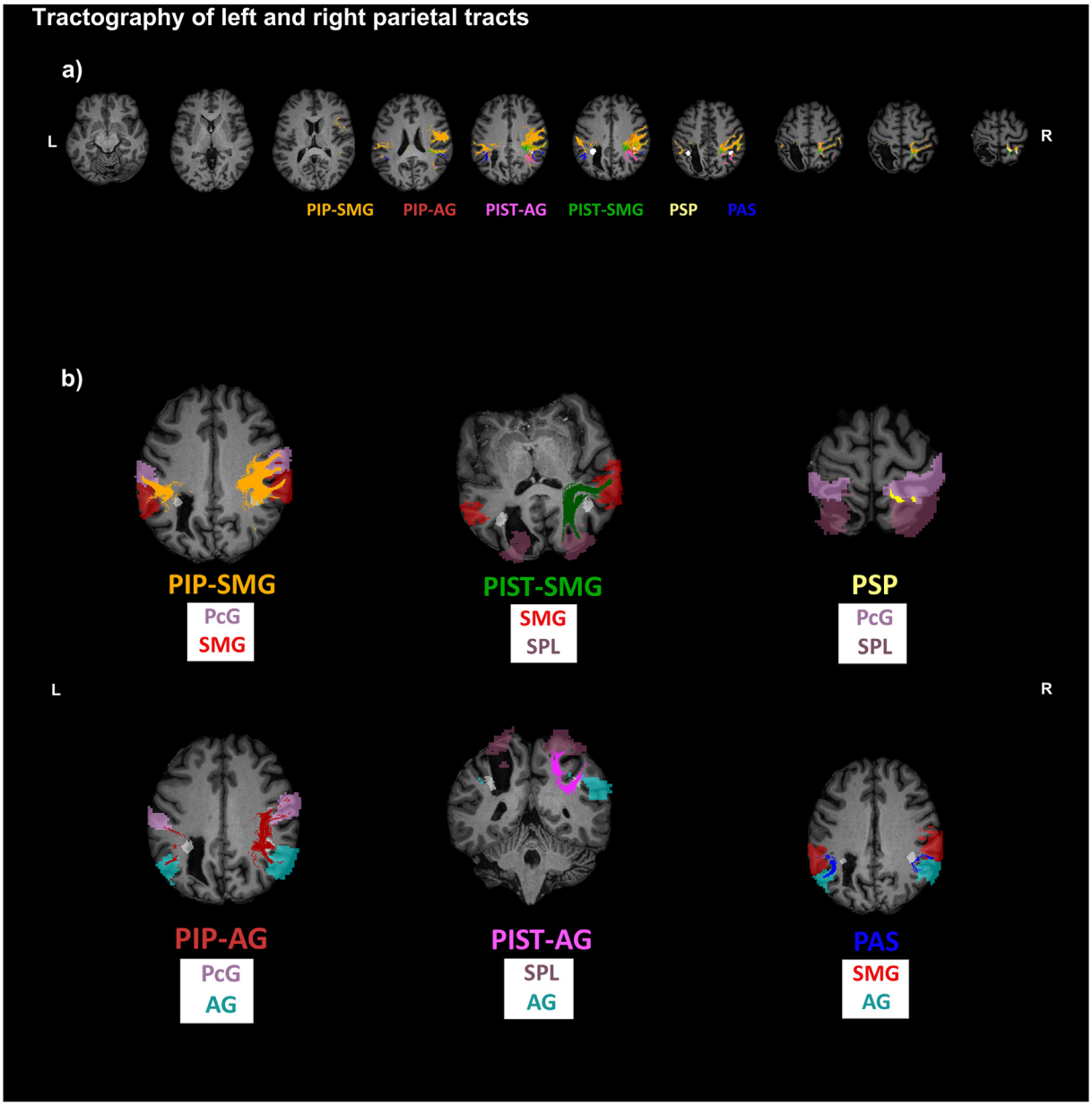

Fig. 4 – Reconstruction of white matter parietal tracts as defined by Catani et al. (2017); see Section 2.2.3 for details, and Fig. 3c for the 3D representation of each tract individually). In each image, the Rusconi ROIs are also plotted in white, within the left and the right hemispheres (see Section 2.2.3, and Fig. 3 for details). However, the fibres were not constrained to pass through the ROI indicated by Rusconi et al. (2009). Panel a: 2D representation of all tracks together (axial view). Panel b: 2D representation of individual tracts (PIP-SMG, PIP-AG, PSP, PAS: axial view; PIST-AG: coronal view; PIST-SMG: customised view), and of tracts starting and ending brain areas (PcG = Post–central gyrus; SPL = Superior Parietal Lobule; SMG = Supramarginal Gyrus; AG = Angular gyrus; PSP = Parietal Superior-to-Postcentral; PIST-SMG = Parietal Inferior-to-Superior Tract, Supramarginal; PIST-AG = Parietal Inferior-to-Superior Tract, Angular; PIP-SMG = Parietal Inferior-to-Postcentral, Supramarginal; PIP-AG= Parietal Inferior-to-Postcentral, Angular; PAS = Parietal Angular-to-Supramarginal).

right PIST-SMG = 808, FA M = .49, SD = .03; left PSP = 0; right PSP = 1323, FA M = .38, SD = .07), and the number of fibre bundles of the PIP-AG and PIP-SMG were considerably reduced in the left lesioned hemisphere as compared to the right healthy one (number of streamlines and FA (M and SD) in: left PIP-AG = 28, FA M = .42, SD = .02; right PIP-AG = 320, FA M = .49, SD = .03; left PIP-SMG = 3117, FA M = .42, SD = .08; right PIP-SMG = 13,553, FA M = .44, SD = .06). Notably, the only tract that was comparable on the left and right hemisphere was the PAS (number of streamlines and FA (M and SD) in: left PAS = 451, FA M = .43, SD = .05; right PAS = 464, FA M = .36, SD = .07).

Table 4 reports for each tract a comparison between the number of streamlines found in the right hemisphere when

Table 4 – The second column from the left reports for each tract the percentage of streamlines found in the left lesioned hemisphere as compared to the healthy right hemisphere (*number of left streamlines/number of right streamlines*) when tractography was computed without considering the ROI defined following Rusconi et al. (2009). A higher percentage indicates a larger number of preserved streamlines in the left lesioned hemisphere in a given tract. The column on the right reports for each tract the percentage of streamlines found in the right (not lesioned) hemisphere when tractography was computed considering the ROI defined following Rusconi et al. (2009) as compared to when such ROI was not considered (*number of right streamlines found considering the Rusconi ROI/number of right streamlines found without considering the Rusconi ROIs*). A higher percentage indicates a larger number of streamlines crossing the Rusconi seed ROI in a given tract.

Parietal Tracts	Number of streamlines in the left/right hemisphere (%) (tractography without the *Rusconi's* seed region)	Number of streamlines with/without the *Rusconi's* seed region in the right hemisphere (%)
PAS	97%	4%
PIST-AG	0%	47%
PIST-SMG	0%	3%
PIP-AG	9%	73%
PIP-SMG	23%	2%
PSP	0%	0%

tractography was computed considering the ROI defined following Rusconi et al. (2009) as compared to when such ROI was not considered. As expected, adding the ROI indicated by Rusconi et al. (2009) as further constraint in the tractography resulted in a reduction of the number of streamlines found in the right hemisphere (number of streamlines in: right PIP-AG = 234, FA *M* = .49, SD = .04; right PIP-SMG = 331, FA *M* = .47, SD = .03; right PIST-AG = 206, FA *M* = .49, SD = .04; right PIST-SMG = 22, FA *M* = .47, SD = .03; right PAS = 18, FA *M* = .47, SD = .04; right PSP = 0), while almost no streamlines crossed the ROI indicated by Rusconi et al. (2009) in the left hemisphere (no streamlines in the left hemisphere for all tract, except one streamline found in the left PIP-SMG).

3. Discussion

The long lasting debate on the origin of GS has led researchers to hypothesise the locus of white matter tracts disconnection causing GS (Rusconi et al., 2009). Following Rusconi and colleagues' works on this matter, however, only few studies have investigated white matter tracts' disconnection underlining this syndrome (Basagni et al., 2021; Papadopoulos et al., 2021). In this case report, we have provided a comprehensive description of the neuroanatomical damage of a left parietal stroke patient suffering from GS. Through lesion mapping and atlas-based estimation of the probability of white matter tracts disconnection (Foulon et al., 2018), we identified the pattern of disconnected tracts characterising this patient. Furthermore, through DTI-based tractography we provided some support to the hypothesis interpreting GS as a disconnection syndrome (Rusconi, 2018; Rusconi et al., 2009, 2010). In what follows, we discuss our case report, summarising the main findings, and highlighting the strengths and limits of our methodological approach.

At the behavioural level, our patient presented all the four symptoms constituting GS: acalculia, finger agnosia, left/right orientation problems, and agraphia. The assessment for the diagnosis of acalculia revealed that the patient specifically suffered from anarithmetia, that is, impairment in number comparison and arithmetic calculation, in absence of transcoding disorders. The assessment for the diagnosis of finger agnosia allowed detecting mild albeit consistent difficulties in finger recognition, neither attributable to finger alexia—our patient could name fingers correctly -, nor to autotopagnosia—our patient could process the location of other body parts. Acalculia, finger agnosia, and left/right orientation problems were assessed through multiple tests and sessions: while the patient's performance was definitely not at floor in these testing sessions, these types of impairment were severe enough to limit the patient's autonomy in everyday life. An anecdote representative of the patient's dramatic condition concerned her awareness of being not able anymore to deal with money in everyday life contexts, and consequently her worries related to the inability to come back working again.

Her worries were also related to her severe optic ataxia, a deficit which is not usually reported in association to GS, but that is consistent with the patient's lesion site, which spread within the superior parietal lobe and extended posteriorly to POJ (Karnath & Perenin, 2005; Perenin & Vighetto, 1988; Pisella et al., 2009). As in our patient, this impairment is usually present in peripheral rather than central vision. Optic ataxia in our patient was particularly severe in grasping with the right (contralesional) hand when the object was presented either on the left or the right side (crossed bilateral optic ataxia: Rondot, de Recondo, & Dumas, 1977). Considering the presence of severe optic ataxia, as well as impairment in executive functioning, visuospatial processing, and object recognition, our patient does not constitute a pure case of GS. The presence of optic ataxia is not customarily assessed in reported cases of GS. Nonetheless, in our patient the GS symptoms were plausibly not the result of co-occurrent deficit. For instance, while previous studies have identified autotopagnosia as potentially interfering with the diagnosis of GS, our patient did not show body-related disorders apart from finger agnosia, and her ability to name fingers and body parts was preserved. Importantly, she did not show any signs of aphasia, which is the most commonly co-occurring impairment of GS (Rusconi et al., 2010), a comorbidity which was a matter of debate for many years (e.g., see Kinsbourne & Warrington, 1963). Also signs of apraxia at experimental testing were negligible, and not detected in the clinical assessment. Taken together, these observations lead us to conclude that in this patient GS likely co-occurred with other

types of unrelated impairment, and that GS symptoms and optic ataxia in our patient co-occurred without however being attributable to a common origin.

As shown through lesion mapping, the lesion was mainly located within the left parietal lobe, from postcentral to superior occipital regions, reaching the inferior parietal lobule and the angular gyrus. The disconnectome analysis and tractography revealed that the lesion caused a large degree of disconnection in both brain regions close to the lesion (intraparietal disconnection), and in far regions (e.g., reaching the occipital and frontal lobes). The extent of disconnection is likely to account for the different types of deficit which were observed in our patient. Specifically, while the GS symptoms are probably due to intraparietal disconnection, disconnection of frontal and occipital areas can account for impairment in cognitive functioning and object recognition, respectively. Importantly, the lesion was within the left superior parietal lobule, while previous studies typically associated GS to damage in and around the left angular gyrus and the supramarginal gyrus (e.g., Mayer et al., 1999; Morris, Luders, Lesser, Dinner, & Hahn, 1984; Tucha, Steup, Smely, & Lange 1997; for revision see: Rusconi et al., 2010). The supramarginal gyrus was not within our patient's lesion, and the lesion only marginally trespassed into the angular region. While we cannot exclude the possibility that the supramarginal gyrus was involved to some extent in the acute phase of stroke, the negligible damage in areas mainly associated to the GS suggests that there is a high probability that in our patient the grey matter regions involved in the four critical abilities where not lesioned but disconnected, thus making of this case a very suited case for testing the Rusconi et al. hypothesis (Rusconi et al., 2009).

Crucially, the lesion reached the border of the white matter area under the inferior parietal lobule indicated by Rusconi et al. (2009) as potential trigger of the GS symptoms. Considering the anatomical localisation of our patient's lesion, it is possible that in our patient the GS symptoms have been triggered by disruption of tracts crossing the small subparietal area identified by Rusconi et al., (2009), causing disconnection in neural areas within the inferior parietal lobule responsible for left/right orientation or numerical abilities, writing and finger knowledge. Critically, one might argue that there is no way to precisely define in our patient the sets of functionally relevant neurons for left/right orientation or numerical abilities, writing and finger knowledge; therefore, we cannot exclude the possibility that these neural areas were lesioned and not uniquely disconnected. While interindividual variability in the localization of brain functions and connections constitutes an important limit of this study (for discussion on this point, see Rusconi et al. (2009)), we should nonetheless acknowledge that none of the coordinates corresponding to individual peaks of activation during calculation, writing, orientation, and finger recognition tasks in the Rusconi et al. 's study (reported in their Fig. 2) fell inside our patient's lesion. This observation further increases the probability that our patient is a case of GS caused by white matter disconnection.

Importantly, DTI-based tractography allowed providing important insight with respect to the disconnection hypothesis advanced by Rusconi et al. (2009). Firstly, tractography of whole-brain fibres crossing the *Rusconi's seed* region remarkably highlighted the dramatic degree of disruption of white matter connections within the left hemisphere as compared to the right one, appearing scarce and gaunt all around the lesion (Fig. 2b). On the contrary, fibres crossing the homologous right-sided seed region constituted a dense network of connections that spread out across the whole hemisphere (Fig. 2b). Secondly, tractography of small parietal tracts described by Catani et al. (2017) indicated that the *Rusconi's* seed region is mainly crossed by tracts connecting the angular gyrus to higher regions of the parietal lobe (i.e., PIST-AG and PIP-AG). Finally, tractography at the level of the parietal lobes also indicated that in our patient parietal the disconnection concerned to a large extent the main part of the reconstructed tracts. This finding is in line with the studies by Papadopoulos et al., (2021) and Basagni et al. (2021), which are very similar in terms of aims to our study. Both studies indeed reported disruption left intraparietal U-fibres in their patients. In particular, Basagni et al. (2021) identified the PAS and the parietal inferior–to–postcentral (PIP) tracts as damaged in their patients. Differently from Basagni et al. (2021), the only tract with appeared to be preserved in our patient was the PAS, further indicating that we can plausibly exclude a critical degree of damage in the angular and the supramarginal gyri. Finally, DTI-based tractography and atlas-based estimation of probability of white matter tracts disconnection provided converging and complementary support to the role of white matter in GS, allowing showing disrupted connections (disconnectome map) as well as sparse preserved connections (DTI-based tractography) within the left hemisphere. In particular, the atlas-based estimation of the probability of white matter tracts disconnection revealed the critical disruption of large parieto-frontal connections, specifically, branches I and II of the left SLF, and left cingulum, once again in line with Papadopoulos et al., (2021) and Basagni et al. (2021) which reported disruption at the level of the left SLF.

In addition, our patient also presented disconnection at the level of the corpus callosum. In the DTI-based tractography we masked the corpus callosum so as to avoid the tracking of the fibres across hemispheres, thus allowing a cross-hemispheric comparison. However, this prevented the assessment of the integrity of the corpus callosum itself. Nonetheless, the probability of disconnection at this site using the atlas-based method for estimation of disconnection was high. Importantly, previous studies discuss the disruption of the posterior part of the corpus callosum–the splenium–in patients with optic ataxia (e.g., Meichtry et al., 2018; Rondot et al., 1977). Recently, Meichtry et al., (2018) investigated white matter tracts disconnection in a patient presenting optic ataxia and visual hemiagnosia following brain damage in the left POJ region, extending to SPL and to the corpus callosum. By means of the same method we used here (Foulon et al., 2018), they found higher-than-chance probability of disconnection in SLF and in the inferior longitudinal fasciculus (ILF), indicating in their patient the presence of a large interplay between the dorsal and the ventral streams. Except for the above-mentioned study by Meichtry et al., (2018), to our knowledge there is currently no systematic investigation of structural connectivity in patients suffering from optic ataxia.

Finally, it is worth noting to mention that, as our patient, none of the two mentioned case reports were pure cases of GS:

the Basagni et al., (2021) presented a variant of GS, given that finger agnosia was accompanied by autotopagnosia; the Papadopoulos et al. (2021) patient presented also impaired comprehension abilities and anomia. Our patient, however, did not show any language or body-schema related impairment. Additionally, the Basagni et al., (2021) showed numerical disorders of the level of transcoding, an ability which was preserved in our patient. The presence or absence of optic ataxia was not reported in these studies. The differences in the manifestation of symptoms might be explained by differences in the lesion site. For instance, the lesion of the Basagni et al., (2021) extended into the SMG and AG while our patient's lesion was mainly located in the superior parietal lobule. As discussed by Basagni et al., (2021), differences in the anatomical localisation of lesions can explain the heterogeneous manifestation of the tetrad symptoms. With this respect, optic ataxia has not frequently been discussed in GS patients (but see Barbosa, Brito, Rodrigues, Kubota, & Parmera, 2017), albeit lesions associated with GS and optic ataxia are probably overlapping to some extent. In this sense, a more comprehensive and systematic neuropsychological assessment covering all the different potential disorders emerging after parietal lobes damage might be beneficial to provide a clear picture of co-occurrence and interactions of different types of impairment (see also: Barbosa et al., 2017).

4. Conclusion

We have described a complete neuroanatomical investigation of a patient suffering from GS following left-parietal brain lesion. The location of the brain lesion only very partially involved the angular gyrus, commonly associated with GS, while including the potentially critical subcortical area indicated by Rusconi et al. (2009). This observation showed that this case study constituted a unique opportunity to test the disconnection hypothesis advanced by Rusconi et al. (2009). By complementing the neuropsychological assessment with the neuroanatomical investigation, we have provided further evidence in favour of the idea that GS can be caused by disruption of subparietal white matter tracts irradiating functionally relevant neural areas within the parietal lobe. Considering the current lack of systematic investigation on white matter tracts disconnection in GS patients, our findings constitute an important added value to this topic. We conclude that the study of white matter tracts disconnection can overcome the limits of the localizationist approach in neuropsychological investigation, offering complementary information to lesion mapping and contributing to explain the heterogeneity of behavioural disorders following brain damage (de Schotten et al., 2014; Forkel et al., 2014).

Authors contribution

Ranzini, M.: Conceptualization, Formal analysis, Methodology, Supervision, Visualization, Writing–original draft, Writing–review & editing D'Imperio, D.: Formal analysis, Investigation, Methodology, Validation, Visualization, Writing–original draft, Writing–review & editing Giustiniani, A.: Investigation, Writing–original draft, Writing–review & editing Danesin, L.: Writing–original draft, Writing–review & editing D'; Antonio, V.: Validation, Writing–review & editing Rigon, E.: Data curation, Investigation, Resources Cacciante, L.: Investigation, Resources Rigon, J.: Data curation, Investigation Meneghello, F.: Investigation, Resources Turolla, A.: Resources, Writing–review & editing Vallesi, A.: Supervision, Writing–review & editing Ferrazzi, G.: Data curation, Formal analysis, Methodology, Software, Visualization, Writing–original draft, Writing–review & editing Semenza, C.: Conceptualization, Methodology, Supervision, Writing–review & editing Burgio, F.: Conceptualization, Project administration, Resources, Supervision, Writing–review & editing.

Acknowledgements

This research was funded by the Italian Ministry of Health, grant number GR-2018-12367927 awarded to F.B. Again, this work was funded by the European Union's Horizon 2020 research and innovation program under Marie Skłodowska-Curie Grant 839394 (to M.R.). We would like to thank Dafnis Batalle (King's College London) for useful discussions.

REFERENCES

Andersson, J. L. R., Skare, S., & Ashburner, J. (2003). How to correct susceptibility distortions in spin-echo echo-planar images: Application to diffusion tensor imaging. *Neuroimage, 20*, 870–888. https://doi.org/10.1016/s1053-8119(03)00336-7

Andersson, J. L., & Sotiropoulos, S. N. (2016). An integrated approach to correction for off-resonance effects and subject movement in diffusion MR imaging. *Neuroimage, 125*, 1063–1078.

Appollonio, I., Leone, M., Isella, V., Piamarta, F., Consoli, T., Villa, M. L., … Nichelli, P. (2005). The frontal assessment battery (FAB): Normative values in an Italian population sample. *Neurological Sciences, 26*(2), 108–116.

Ardila, A. (2020). Gerstmann syndrome. *Current Neurology and Neuroscience Reports, 20*(11), 1–5.

Ardila, A., Concha, M., & Rosselli, M. (2000). Angular gyrus syndrome revisited: Acalculia, finger agnosia, right-left disorientation and semantic aphasia. *Aphasiology, 14*(7), 743–754.

Barbosa, B. J. A. P., Brito, M. H. D., Rodrigues, J. C., Kubota, G. T., & Parmera, J. B. (2017). Gerstmann's syndrome and unilateral optic ataxia in the emergency department. *Dementia & Neuropsychologia, 11*, 459–461.

Basagni, B., Luzzatti, C., De Tanti, A., Bozzetti, F., Crisi, G., Pinardi, C., … Fogassi, L. (2021). Some evidence on Gerstmann's syndrome: A case study on a variant of the clinical disorder. *Brain and Cognition, 148*, Article 105679.

Benton, A. L. (1992). Gerstmann's syndrome. *Archives of neurology, 49*(5), 445–447.

Benton, A. L., Varney, N. R., & Hamsher, K. D. (1983). *Judgment of line orientation*.

Berlucchi, G., & Vallar, G. (2018). The history of the neurophysiology and neurology of the parietal lobe. *Handbook of clinical neurology, 151*, 3–30.

Borchers, S., Müller, L., Synofzik, M., & Himmelbach, M. (2013). Guidelines and quality measures for the diagnosis of optic ataxia. *Frontiers in human neuroscience, 7*, 324.

Budisavljevic, S., Dell'Acqua, F., & Castiello, U. (2018). Cross-talk connections underlying dorsal and ventral stream integration during hand actions. *Cortex; a Journal Devoted To the Study of the Nervous System and Behavior, 103*, 224–239.

Burgio, F., Danesin, L., Benavides-Varela, S., Meneghello, F., Butterworth, B., Arcara, G., et al. (2022). Numerical activities of daily living: A short version. *Neurological Sciences, 43*(2), 967–978.

Caffarra, P., Vezzadini, G., Dieci, F., Zonato, F., & Venneri, A. (2002a). Una versione abbreviata del test di Stroop: Dati normativi nella popolazione italiana. *Nuova Rivista di Neurologia, 12*(4), 111–115.

Caffarra, P., Vezzadini, G., Dieci, F., Zonato, F., & Venneri, A. (2002b). Rey-osterrieth complex figure: Normative values in an Italian population sample. *Neurological sciences, 22*(6), 443–447.

Caffarra, P., Vezzadini, G., Dieci, F., Zonato, F., & Venneri, A. (2004). Modified card sorting test: Normative data. *Journal of Clinical and Experimental Neuropsychology, 26*(2), 246–250.

Carlesimo, G. A., Caltagirone, C., Gainotti, G. U. I. D., Fadda, L., Gallassi, R., Lorusso, S., … Parnetti, L. (1996). The mental deterioration battery: Normative data, diagnostic reliability and qualitative analyses of cognitive impairment. *European neurology, 36*(6), 378–384.

Carota, A., Di Pietro, M., Ptak, R., Poglia, D., & Schnider, A. (2004). Defective spatial imagery with pure Gerstmann's syndrome. *European Neurology, 52*(1), 1–6.

Catani, M., Robertsson, N., Beyh, A., Huynh, V., de Santiago Requejo, F., Howells, H., … Dell'Acqua, F. (2017). Short parietal lobe connections of the human and monkey brain. *Cortex; a Journal Devoted To the Study of the Nervous System and Behavior, 97*, 339–357.

Cattelani, R., Dal Sasso, F., Corsini, D., & Posteraro, L. (2011). The modified five-point test: Normative data for a sample of Italian healthy adults aged 16–60. *Neurological Sciences, 32*(4), 595–601.

de Haan, B., Clas, P., Juenger, H., Wilke, M., & Karnath, H.-O. (2015). Fast semi-automated lesion demarcation in stroke. *NeuroImage: Clinical, 9*, 69–74. https://doi.org/10.1016/j.nicl.2015.06.013

De Renzi, E., Pieczuro, A., & Vignolo, L. A. (1968). Ideational apraxia: A quantitative study. *Neuropsychologia, 6*(1), 41–52.

de Schotten, T.,M., Tomaiuolo, F., Aiello, M., Merola, S., Silvetti, M., Lecce, F., … Doricchi, F. (2014). Damage to white matter pathways in subacute and chronic spatial neglect: A group study and 2 single-case studies with complete virtual "in vivo" tractography dissection. *Cerebral cortex, 24*(3), 691–706.

D'Imperio, D., Tomelleri, G., Moretto, G., & Moro, V. (2017). Modulation of somatoparaphrenia following left-hemisphere damage. *Neurocase, 23*(2), 162–170.

Dulyan, L., Talozzi, L., Pacella, V., Corbetta, M., Forkel, S. J., & Thiebaut de Schotten, M. (2022). Longitudinal prediction of motor dysfunction after stroke: A disconnectome study. *Brain Structure & Function, 227*, 3085–3098.

Forkel, S. J., Thiebaut de Schotten, M., Dell'Acqua, F., Kalra, L., Murphy, D. G., Williams, S. C., et al. (2014). Anatomical predictors of aphasia recovery: A tractography study of bilateral perisylvian language networks. *Brain: a Journal of Neurology, 137*(7), 2027–2039.

Foulon, C., Cerliani, L., Kinkingnehun, S., Levy, R., Rosso, C., Urbanski, M., … Thiebaut de Schotten, M. (2018). Advanced lesion symptom mapping analyses and implementation as BCBtoolkit. *Gigascience, 7*(3), giy004.

Gerstmann, J. (1924). Fingeragnosie-Eine umschriebene Storung der Orientierung am eigenen Korper. *Wiener Klinische Wochenschrift, 37*, 1010–1012.

Gerstmann, J. (1927). Fingeragnosie und isolierte Agraphie—ein neues Syndrom. *Zeitschrift für die gesamte Neurologie und Psychiatrie, 108*, 152–177.

Gerstmann, J. (1930). Zur Symptomatologie der Herderkrankimgen in der Übergangsregion der unteren Parietal-und mittleren Okzipitalhirnwindung. *Deutsche Zeitschrift für Nervenheilkunde, 116*, 46–49.

Giovagnoli, A. R., Del Pesce, M., Mascheroni, S., Simoncelli, M., Laiacona, M., & Capitani, E. (1996). Trail making test: Normative values from 287 normal adult controls. *The Italian journal of neurological sciences, 17*(4), 305–309.

Giustiniani, A., Danesin, L., Ranzini, M., D'Imperio, D., Rigon, J., Ferrazzi, G., et al. (2022). *A new approach in the treatment of optic ataxia: Evidence from a single case study*. Poster session presentation *at the European workshop on cognitive neuropsychology*. Brixen: IT.

Goodale, M. A., & Milner, A. D. (1992). Separate visual pathways for perception and action. *Trends in neurosciences, 15*(1), 20–25.

Hayashi, Y., Kinoshita, M., Furuta, T., Watanabe, T., Nakada, M., & Hamada, J. I. (2013). Right superior longitudinal fasciculus: Implications for visuospatial neglect mimicking Gerstmann's syndrome. *Clinical Neurology and Neurosurgery, 115*(6), 775–777.

Heimburger, R. F., Demyer, W., & Reitan, R. M. (1964). Implications of Gerstmann's syndrome. *Journal of Neurology, Neurosurgery, and Psychiatry, 27*(1), 52.

Herrmann, G., & Pötzl, O. (1926). *Über die Agraphie und ihre lokaldiagnostischen Beziehungen*. Karger Publishers.

João, R. B., Filgueiras, R. M., Mussi, M. L., & Barros, J. E. F. D. (2017). Transient Gerstmann syndrome as manifestation of stroke: Case report and brief literature review. *Dementia & Neuropsychologia, 11*, 202–205.

Karnath, H.-O., & Perenin, M.-T. (2005). Cortical control of visually guided reaching: Evidence from patients with optic ataxia. *Cerebral Cortex, 15*(10), 1561e1569.

Kinsbourne, M., & Warrington, E. K. (1963). The developmental Gerstmann syndrome. *Archives of Neurology, 8*(5), 490–501.

Kleinschmidt, A., & Rusconi, E. (2011). Gerstmann meets Geschwind: A crossing (or kissing) variant of a subcortical disconnection syndrome? *The Neuroscientist: a Review Journal Bringing Neurobiology, Neurology and Psychiatry, 17*(6), 633–644.

Levin, M. F., Desrosiers, J., Beauchemin, D., Bergeron, N., & Rochette, A. (2004). Development and validation of a scale for rating motor compensations used for reaching in patients with hemiparesis: The reaching performance scale. *Physical therapy, 84*(1), 8–22.

Magni, E., Binetti, G., Bianchetti, A., Rozzini, R., & Trabucchi, M. (1996). Mini-mental state examination: A normative study in Italian elderly population. *European Journal of Neurology, 3*(3), 198–202.

Mayer, E., Martory, M. D., Pegna, A. J., Landis, T., Delavelle, J., & Annoni, J. M. (1999). A pure case of Gerstmann syndrome with a subangular lesion. *Brain: a Journal of Neurology, 122*(6), 1107–1120.

Mazzoni, M., Pardossi, L., Cantini, R., Giorgetti, V., & Arena, R. (1990). Gerstmann syndrome: A case report. *Cortex; a Journal Devoted To the Study of the Nervous System and Behavior, 26*(3), 459–467.

Meichtry, J. R., Cazzoli, D., Chaves, S., von Arx, S., Pflugshaupt, T., Kalla, R., … Müri, R. M. (2018). Pure optic ataxia and visual hemiagnosia—extending the dual visual hypothesis. *Journal of neuropsychology, 12*(2), 271–290.

Miceli, G., & Capasso, R. (1991). *I disturbi del calcolo: Diagnosi e riabilitazione*. Milano: Masson.

Monaco, M., Costa, A., Caltagirone, C., & Carlesimo, G. A. (2013). Forward and backward span for verbal and visuo-spatial data: Standardization and normative data from an Italian adult population. *Neurological Sciences, 34*(5), 749–754.

Moro, V., Pernigo, S., Urgesi, C., Zapparoli, P., & Aglioti, S. M. (2009). Finger recognition and gesture imitation in Gerstmann's syndrome. *Neurocase, 15*(1), 13–23.

Morris, H. H., Luders, H., Lesser, R. P., Dinner, D. S., & Hahn, J. (1984). Transient neuropsychological abnormalities (including Gerstmann's Syndrome) during cortical stimulation. *Neurology, 34*(7), 877, 877.

Novelli, G., Papagno, C., Capitani, E., & Laiacona, M. (1986). *Tre test clinici di ricerca e produzione lessicale. Taratura su sogetti normali.* Archivio di psicologia, neurologia e psichiatria.

Pacella, V., Scandola, M., Beccherle, M., Bulgarelli, C., Avesani, R., Carbognin, G., … Moro, V. (2020). Anosognosia for theory of mind deficits: A single case study and a review of the literature. *Neuropsychologia, 148*, Article 107641.

Papadopoulos, V. E., Tsatsou, K., Toulas, P., Christidi, F., Karavasilis, E., Angelopoulou, M. K., et al. (2021). Gerstmann syndrome as a disconnection syndrome, evidence from DTI tractography: A case report. *Journal of Neurolinguistics, 57*, Article 100955.

Patil, V. C., & Kulkarni, A. R. (2019). Gerstmann's syndrome: A rare clinical condition with a tetrad of symptoms. *Ratio, 12*, 1, 1.

Perenin, M. T., & Vighetto, A. (1988). Optic ataxia: A specific disruption in visuomotor mechanisms: I. Different aspects of the deficit in reaching for objects. *Brain: a Journal of Neurology, 111*(3), 643–674.

Pisella, L., Sergio, L., Blangero, A., Torchin, H., Vighetto, A., & Rossetti, Y. (2009). Optic ataxia and the function of the dorsal stream: Contributions to perception and action. *Neuropsychologia, 47*(14), 3033–3044.

Poeck, K., & Orgass, B. (1966). Gerstmann's syndrome and aphasia. *Cortex; a Journal Devoted To the Study of the Nervous System and Behavior, 2*(4), 421–437.

Ranzini, M., Scarpazza, C., Radua, J., Cutini, S., Semenza, C., & Zorzi, M. (2022). A common neural substrate for number comparison, hand reaching and grasping: A SDM-PSI meta-analysis of neuroimaging studies. *Cortex; a Journal Devoted To the Study of the Nervous System and Behavior, 148*, 31–67.

Raven, J. C., & Court, J. H. (1990). *Manual for Raven's progressive matrices and vocabulary scales*. section 2(: coloured progressive matrices).

Roeltgen, D. P., & Heilman, K. M. (1985). Review of agraphia and a proposal for an anatomically-based neuropsychological model of writing. *Applied Psycholinguistics, 6*(3), 205–229.

Rolls, E. T., Huang, C. C., Lin, C. P., Feng, J., & Joliot, M. (2020). Automated anatomical labelling atlas 3. *Neuroimage, 206*, Article 116189.

Rolls, E. T., Joliot, M., & Tzourio-Mazoyer, N. (2015). Implementation of a new parcellation of the orbitofrontal cortex in the automated anatomical labeling atlas. *Neuroimage, 122*, 1–5.

Rondot, P., de Recondo, J., & Dumas, J. L. (1977). Visuomotor ataxia. *Brain: a Journal of Neurology, 100*, 355–376.

Rorden, C. (2019). *Mricron [computer software] vo 1.0* (Version 1.0.20190902).

Rorden, C., & Brett, M. (2000). Stereotaxic display of brain lesions. *Behavioural neurology, 12*(4), 191–200.

Rossetti, Y., Pisella, L., & McIntosh, R. D. (2019). Definition: Optic ataxia. *Cortex; a Journal Devoted To the Study of the Nervous System and Behavior, 121*, 481.

Rourke, B. P., & Conway, J. A. (1997). Disabilities of arithmetic and mathematical reasoning: Perspectives from neurology and neuropsychology. *Journal of Learning Disabilities, 30*(1), 34–46.

Rusconi, E. (2018). Gerstmann syndrome: Historic and current perspectives. *Handbook of clinical neurology, 151*, 395–411.

Rusconi, E., & Cubelli, R. (2019). The making of a syndrome: The English translation of Gerstmann's first report. *Cortex; a Journal Devoted To the Study of the Nervous System and Behavior, 117*, 277–283.

Rusconi, E., Pinel, P., Dehaene, S., & Kleinschmidt, A. (2010). The enigma of gerstmann's syndrome revisited: A telling tale of the vicissitudes of neuropsychology. *Brain: a Journal of Neurology, 133*(2), 320–332.

Rusconi, E., Pinel, P., Eger, E., LeBihan, D., Thirion, B., Dehaene, S., et al. (2009). A disconnection account of gerstmann syndrome: Functional neuroanatomy evidence. *Annals of Neurology: Official Journal of the American Neurological Association and the Child Neurology Society, 66*(5), 654–662.

Santangelo, G., Siciliano, M., Pedone, R., Vitale, C., Falco, F., Bisogno, R., … Trojano, L. (2015). Normative data for the montreal cognitive assessment in an Italian population sample. *Neurological Sciences, 36*(4), 585–591.

Sauguet, J., Benton, A. L., & Hecaen, H. (1971). Disturbances of the body schema in relation to language impairment and hemispheric locus of lesion. *Journal of Neurology, Neurosurgery, and Psychiatry, 34*(5), 496–501.

Sheimo, D. L., Bardach, L. G., & Hilfinger, P. (1997). Fluent aphasia with gerstmann's syndrome: A case study. *Aphasiology, 11*(3), 283–291.

Sim, E. J., Helbig, H. B., Graf, M., & Kiefer, M. (2015). When action observation facilitates visual perception: Activation in visuo-motor areas contributes to object recognition. *Cerebral cortex, 25*(9), 2907–2918.

Smith, R. E., Tournier, J.-D., Calamante, F., & Connelly, A. (2012). Anatomically-constrained tractography: Improved diffusion MRI streamlines tractography through effective use of anatomical information. *Neuroimage, 62*, 1924–1938.

Spinnler, H., & Tognoni, G. (1987). Gruppo italiano per lo studio neuropsicologico dell'invecchiamento. Standardizzazione e taratura italiana di test neuropsicologici. *Ital J Neurol Sci, 6*(Suppl 8), 1–120.

Stengel, E. (1944). Loss of spatial orientation, constructional apraxia and Gerstmann's syndrome. *Journal of Mental Science, 90*(380), 753–760.

Strub, R., & Geschwind, N. (1974). Gerstmann syndrome without aphasia. *Cortex; a Journal Devoted To the Study of the Nervous System and Behavior, 10*(4), 378–387.

Tanabe, N., Komuro, T., Mochida, A., Fujita, Y., Nakagawa, M., Hyuga, J., … Satow, T. (2020). A case of inferior frontal gyrus infarction manifesting Gerstmann syndrome. *Neurocase, 26*(6), 368–371.

Tessari, A., Toraldo, A., Lunardelli, A., Zadini, A., & Rumiati, R. I. (2015). STIMA: A short screening test for ideo-motor apraxia, selective for action meaning and bodily district. *Neurological Sciences, 36*(6), 977–984.

Tournier, J. D., Smith, R., Raffelt, D., Tabbara, R., Dhollander, T., Pietsch, M., … Connelly, A. (2019). MRtrix3: A fast, flexible and open software framework for medical image processing and visualisation. *Neuroimage, 202*, Article 116137.

Tournier, J. D., Yeh, C. H., Calamante, F., Cho, K. H., Connelly, A., & Lin, C. P. (2008). Resolving crossing fibres using constrained spherical deconvolution: Validation using diffusion-weighted imaging phantom data. *Neuroimage, 42*(2), 617–625.

Tucha, O., Steup, A., Smely, C., & Lange, K. W. (1997). Toe agnosia in Gerstmann syndrome. *Journal of Neurology, Neurosurgery, and Psychiatry, 63*(3), 399–403.

Veraart, J., Novikov, D. S., Christiaens, D., Ades-Aron, B., Sijbers, J., & Fieremans, E. (2016). Denoising of diffusion MRI using random matrix theory. *Neuroimage, 142*, 394–406. https://doi.org/10.1016/j.neuroimage.2016.08.016

Warrington, E. K., & James, M. (1991). *VOSP: The visual object and space perception battery*. Pearson.

Yushkevich, P. A., Piven, J., Hazlett, H. C., Smith, R. G., Ho, S., Gee, J. C., et al. (2006). User-guided 3D active contour segmentation of anatomical structures: Significantly improved efficiency and reliability. *Neuroimage, 31*(3), 1116–1128.

Zorzi, M., Priftis, K., & Umiltà, C. (2002). Neglect disrupts the mental number line. *Nature, 417*(6885), 138–139.